Acta Crystallographica Section F
Structural Biology and Crystallization Communications
ISSN 1744-3091

Cloning, purification, crystallization and preliminary X-ray analysis of the receiver domain of the histidine kinase CKI1 from *Arabidopsis thaliana*

Tomáš Klumpler, Blanka Pekárová, Jaromír Marek,* Petra Borkovcová, Lubomír Janda and Jan Hejátko

Laboratory of Molecular Plant Physiology, Department of Functional Genomics and Proteomics, Institute of Experimental Biology, Faculty of Science, Masaryk University, Kamenice 5/A2, CZ-625 00 Brno, Czech Republic

Correspondence e-mail: marek@chemi.muni.cz

Received 15 January 2009
Accepted 31 March 2009

The receiver domain (RD) of a sensor histidine kinase (HK) catalyses the transphosphorylation reaction during the action of HKs in hormonal and abiotic signalling in plants. Crystals of the recombinant RD of the *Arabidopsis thaliana* HK CYTOKININ-INDEPENDENT1 ($CKI1_{RD}$) have been obtained by the hanging-drop vapour-diffusion method using ammonium sulfate as a precipitant and glycerol as a cryoprotectant. The crystals diffracted to approximately 2.4 Å resolution on beamline BW7B of the DORIS-III storage ring. The diffraction improved significantly after the use of a non-aqueous cryoprotectant. Crystals soaked in Paratone-N diffracted to at least 2.0 Å resolution on beamline BW7B and their mosaicity decreased more than tenfold. The crystals belonged to space group $C222_1$, with unit-cell parameters a = 54.46, b = 99.82, c = 79.94 Å. Assuming the presence of one molecule of the protein in the asymmetric unit gives a Matthews coefficient V_M of 2.33 Å^3 Da^{-1}. A molecular-replacement solution has been obtained and structure refinement is in progress.

1. Introduction

Sensor histidine kinases (HKs) are members of the two-component (TC) signalling systems that mediate signal transduction in a broad spectrum of adaptive responses in bacteria (Calva & Oropeza, 2006; Hoch, 2000). A modified version of bacterial TC signalling has been adapted by yeast and plants (Chang & Stewart, 1998): as a so-called two-component phosphorelay (Hoch, 2000). In TC signalling in plants, the membrane-associated sensor HK interacts with a signalling molecule, which activates an intracellular HK domain and leads to autophosphorylation of its conserved histidine moiety. The downstream phosphorelay is initiated by a receiver domain (RD) of the HK. The RD transfers phosphate from a His to its own Asp and further transmits the signal *via* transphosphorylation to the His of a histidine-containing phosphotransfer (HPt) domain. The HPt proteins translocate the signal to the nucleus, where the phosphorylated histidine serves as a donor for the phosphorylation of a final phosphate acceptor, the Asp residue of the response regulator (To & Kieber, 2008; Mizuno, 2005).

The receiver domain of sensor HKs seems to mediate the limiting steps in the above-described phosphorelay and thus signal transduction. In addtion to its catalytic activity, which triggers the phosphorelay, the RD is also supposed to be involved in specific protein–protein interactions with its downstream signalling partners. The amino-acid residues in the C-terminal domains of the sensor HKs have recently been shown to be responsible for the specificity of the signal transduction to their downstream signalling proteins in bacteria (Skerker *et al.*, 2008). Moreover, the amino acids predicted, using covariant analysis, to be important for the specific protein–protein interactions were located close to the physical interface of both interaction partners (Skerker *et al.*, 2008). This suggests that the structure of the RD might contribute to the recognition of its interaction partner(s).

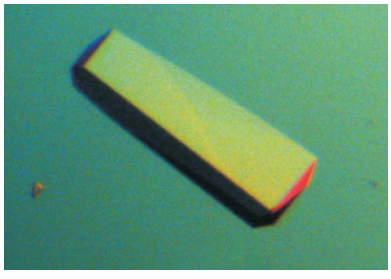

In the *Arabidopsis thaliana* genome, genes encoding 11 HKs, six HPt proteins and 23 response regulators have been identified. *A. thaliana* HKs mediate discrete responses to various phytohormones (ethylene, cytokinin and abscisic acid) and abiotic stress (osmosensing) (Mizuno, 2005; Tran *et al.*, 2007). Based on the mechanism of the above-described bacterial TC signalling, protein–protein interactions of the RD domains of individual histidine kinases and HPt proteins will presumably be involved in determination of the specificity of the individual signalling pathways and/or their crosstalk in plants. However, the mechanisms discriminating this specificity at the protein level, which are likely to depend on differential tertiary structures of the interacting partners, have not yet been characterized. Thus, knowledge of the structure of individual RDs and their interaction partners seems to be critical to our understanding of the molecular mechanism of these specific interactions. To date, the structures of many bacterial RDs belonging to a family of phosphatases and phosphate carrier proteins have been determined, *e.g.* CheY (Stock *et al.*, 1989) and PhoB (Sola *et al.*, 1999). However, the RD of ethylene receptor ETR1 is the only receiver domain from a plant for which the structure has been solved (Muller-Dieckmann *et al.*, 1999).

The sensor histidine kinase CKI1 was identified as an activator of a cytokinin-like response when overexpressed in hypocotyl explants of *A. thaliana* (Kakimoto, 1996). However, in contrast to the genuine cytokinin receptors of *A. thaliana*, AHK2, AHK3 and AHK4, CKI1 was found to be constitutively active in bacteria and yeast or *A. thaliana* protoplasts (Yamada *et al.*, 2001; Hwang & Sheen, 2001). Thus, the specificity and the role of CKI1 in the TC signalling in *A. thaliana* remain unclear. Our recent data suggest that $CKI1_{RD}$ is responsible for a specific interaction with individual HPt proteins in *A. thaliana* (Pekárová *et al.*, manuscript in preparation). Here, we describe the cloning, protein overproduction, purification, crystallization and preliminary X-ray diffraction analysis of $CKI1_{RD}$ from *A. thaliana*.

2. Materials and methods

2.1. Cloning and protein overproduction

A plasmid containing a DNA fragment encoding the receiver domain of CKI1 ($CKI1_{RD}$) was generated by PCR using *CKI1* cDNA (provided by T. Kakimoto, Osaka University, Japan) as a template and primers 5′-TAA TG**G CTA GC**A CAG ATT CAG AGA GT-3′ (*Nhe*I restriction site in bold) and 5′-TAT AC**C TCG AG**A GTG ACG TTT GCT TTC GAT TTC TC-3′ (*Xho*I restriction site in bold).

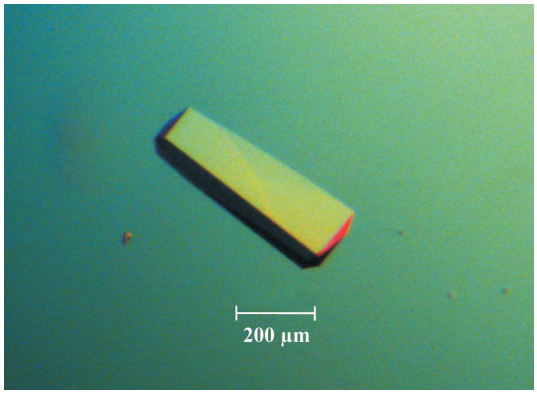

Figure 1
An example of a typical crystal of $CKI1_{RD}$.

The amplified DNA fragment was purified on agarose gel, digested with *Nhe*I and *Xho*I, ligated into the vector pET28a(+) (Novagen) and transformed into *Escherichia coli* strain DH10β and finally into *E. coli* strain BL21(DE3)pLysS. The cells carrying the expression plasmid were cultured with shaking in TB medium pH 7.5 at 310 K until an OD_{600} of 0.8 was reached. At this point, the expression of $CKI1_{RD}$ was induced by adding isopropyl β-D-1-thiogalactopyranoside to a final concentration of 0.42 m*M*. After 3 h incubation at 301 K, the cells were harvested by centrifugation at 3500*g* for 20 min at 277 K.

2.2. Purification

The cells expressing $CKI1_{RD}$ were resuspended in a buffer containing 20 m*M* Tris–HCl pH 7.9, 500 m*M* NaCl, 0.1% Triton X-100 and disintegrated by sonication. After centrifugation at 48 500*g* for 40 min at 277 K, the supernatant was applied onto a HiTrap Chelating HP column (Amersham Biosciences, ÄKTA FPLC system) charged with Zn^{2+} ions and equilibrated in 50 m*M* Tris–HCl pH 7.0, 1 *M* NaCl, 20 m*M* imidazole. The protein was eluted with a linear gradient of imidazole (20–150 m*M*) and pH (7.0–4.5).

The final purification was achieved by gel filtration with a HiLoad 16/60 Superdex 75 prep-grade column (Amersham Biosciences, ÄKTA FPLC system) equilibrated in 50 m*M* Tris–HCl pH 7.5, 150 m*M* NaCl, 10 m*M* EDTA. The collected fractions were analysed on polyacrylamide gels. SDS–PAGE and native PAGE were performed according to Laemmli (1970) using 15%(*w*/*v*) separation gels. Pure fractions (≥95%, Densitometer GS-800, *Quantity One 1-D* analysis software; Bio-Rad) were concentrated to a final concentration of 10 mg ml^{-1} using an Amicon Ultra system (Millipore) with a molecular-weight cutoff of 10 kDa. The protein concentration was determined according to Bradford (1976) using BSA as a standard. The purified protein was stored at 277 K temporarily and at 193 K for long-term storage.

2.3. Crystallization

Preliminary screening of crystallization conditions was carried out by the sitting-drop (100 nl protein solution mixed with 100 nl reservoir solution equilibrated against 100 µl reservoir solution) vapour-diffusion method at 293 K in 96-well plates using an automated nanolitre liquid-handling system (Mosquito, TTP LabTech) and Structure Screen I + II HT-96, MemStart + MemSys HT-96 and PACT Premier HT-96 (all screens were from Molecular Dimensions). Promising microcrystals were obtained after a few days from condition A5 of the MemStart + MemSys screen (0.1 *M* sodium acetate buffer pH 4.6, 2.0 *M* ammonium sulfate). The gradual optimization of the identified conditions was focused on increasing the drop and crystal size, improvement of crystal quality and the use of cryoprotectant. The optimization yielded an optimized composition of the reservoir solution consisting of 2.54 *M* ammonium sulfate, 15.9%(*v*/*v*) glycerol and 0.1 *M* MES buffer pH 5.05. Crystals (Fig. 1) of maximum dimensions of up to 800 × 250 × 50 µm were obtained within 2–3 d in 24-well plates using the hanging-drop vapour-diffusion method with drops containing 1 µl protein solution mixed with 1 µl reservoir solution and equilibrated against 1000 µl reservoir solution at 293 K.

2.4. Data collection and processing

For the collection of the first data set, the crystals were transferred from mother liquor containing 16%(*v*/*v*) glycerol directly into a cold nitrogen stream (100 K) on beamline BW7B of the DORIS-III storage ring at EMBL/DESY (Hamburg, Germany). For the collec-

Table 1
Data-collection statistics.

Values in parentheses are for the highest resolution shell. Observed reflections are those for which $I > 2\sigma(I)$.

Cryoprotectant	Glycerol	Glycerol + Paratone-N
Mosaicity (°)	0.577	0.04
Resolution range (Å)	19.3–2.24 (2.37–2.24)	19.4–2.00 (2.07–2.00)
Completeness (all/observed) (%)	98.3/75.8 (97.7/54.7)	99.8/90.7 (99.9/76.9)
Reflections (all/observed)	71472/55981 (9554/5523)	167628/156406 (10541/8238)
Unique reflections (all/observed)	10396/8016 (1578/884)	15054/13674 (1439/1107)
$I/\sigma(I)$ (all/observed)	15.8/20.5 (4.2/7.3)	20.6/22.6 (7.2/9.2)
$R_{\rm merge}$† (all/observed) (%)	9.2/7.6 (48.9/30.3)	9.5/9.2 (32.3/26.2)

† $R_{\rm merge} = \sum_{hkl}\sum_i |I_i(hkl) - \langle I(hkl)\rangle| / \sum_{hkl}\sum_i I_i(hkl)$, where $I_i(hkl)$ is the intensity of reflection hkl and $\sum_i$ is the sum over all i measurements of reflection hkl.

tion of the second data set, the crystals were flash-cooled to 100 K after soaking in the cryoprotectant Paratone-N (Molecular Dimensions). All data frames were collected at a wavelength of 0.8423 Å using a MAR345 image-plate detector (MAR Research) in dose mode with an oscillation angle of 1.0°. Data for the second set with Paratone-N were recorded in two sweeps at different distances and doses in order to accurately record both the strongest low-resolution and the weakest high-resolution diffraction intensities. A total of 180 images were collected during each of the sweeps. All data were processed and merged using the *XDS* system (Kabsch, 1993). The data-collection statistics are summarized in Table 1.

3. Results and discussion

As shown in Fig. 2(*a*) and Table 1, the diffraction images of the crystal of $CKI1_{RD}$ with the 'natural' cryoprotectant glycerol showed significant widening (the *XDS* package interpreted this widening as a mosaicity of 0.6°) and a corresponding attenuation of the diffraction spots around 3.0 Å resolution. The diffraction images changed dramatically after the use of the non-aqueous cryoprotectant Paratone-N. The widening of the spots disappeared (see Fig. 2*b*), the mosaicity decreased more than tenfold (to a value of 0.04° in *XDS*) and the resolution of the data increased to at least 2.0 Å.

The crystal of $CKI1_{RD}$ belonged to the orthorhombic *C*-centric space group $C222_1$, with unit-cell parameters a = 54.46, b = 99.82, c = 79.94 Å. Assuming that the asymmetric unit contains one molecule of the protein gives a Matthews coefficient V_M of 2.33 Å^3 Da^{-1} (Matthews, 1968); the estimated solvent content is then approximately 47.3%.

The structure of $CKI1_{RD}$ was determined by molecular replacement using an automated scheme for molecular replacement as implemented in *MrBUMP* v.0.4.1 (Keegan & Winn, 2007) in conjunction with the multiple sequence-alignment program *T-Coffee* (Notredame *et al.*, 2000), with *Phaser* (McCoy *et al.*, 2007) as the molecular-replacement engine and *REFMAC* (Murshudov *et al.*, 1997) as the refinement program. An unambiguous solution was found using the bacterial response-regulator protein CheY (PDB entry 1ab5; Wilcock *et al.*, 1998) as a search model. It gave an initial R value of 0.54, which decreased to R = 0.413 and $R_{\rm free}$ = 0.426 after 30 cycles of *REFMAC* refinement. The quality of the $2F_o - F_c$ map generated with this result was good enough to allow successful application of the autobuild regime of *ARP/wARP* (v.7.0.1; Cohen *et al.*, 2008). Model improvement and refinement based on both X-ray and NMR data (Pekárová *et al.*, unpublished data) is in progress.

This work was supported by the Ministry of Education, Youth and Sports of the Czech Republic (grant Nos. MSM0021622415 and LC06034). We wish to thank the staff at EMBL Hamburg for their assistance with data collection on beamline BW7B of the DORIS-III storage ring at DESY Hamburg, the EMBL/DESY Hamburg for

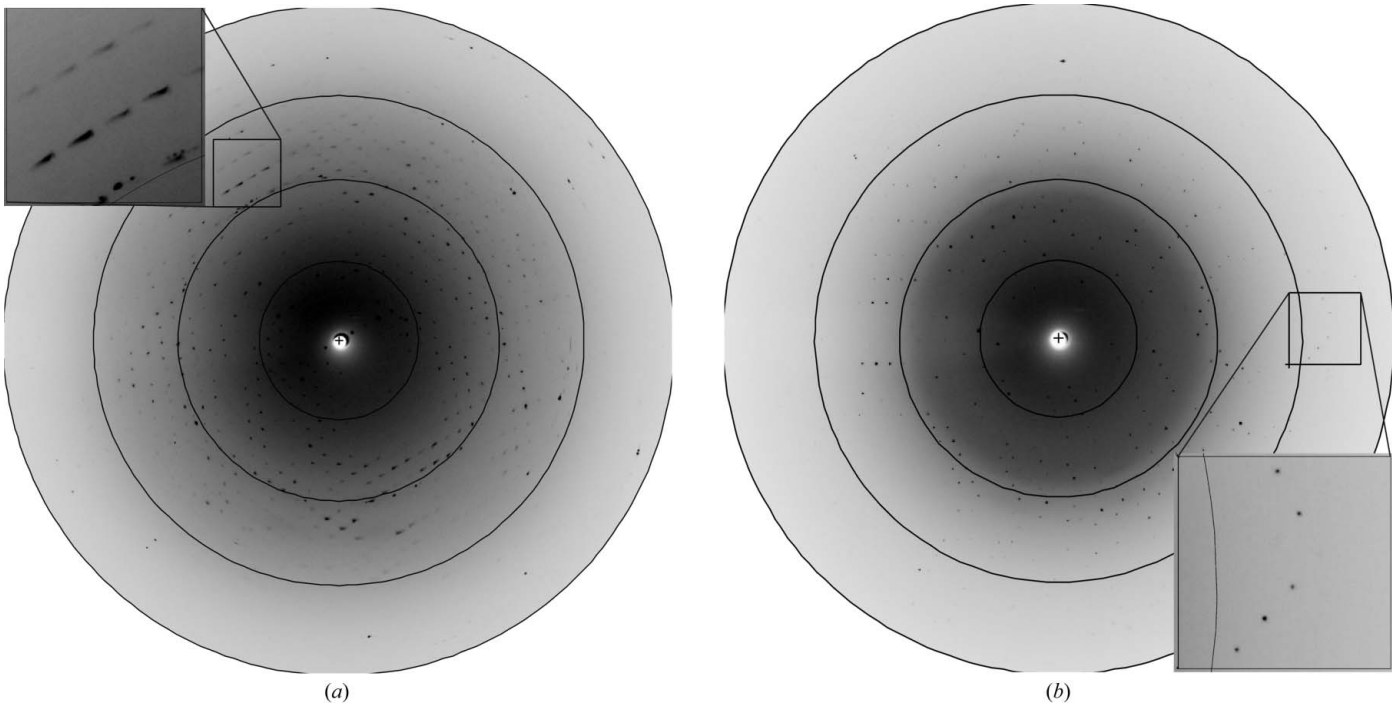

Figure 2
Representative 1.0° oscillation images of the data collected from a $CKI1_{RD}$ crystal using a MAR345 image-plate detector on station BW7B of the DORIS-III storage ring at DESY Hamburg. (*a*) An image from an unsoaked crystal of $CKI1_{RD}$. The magnified rectangle shows a typical example of the widening of the diffraction spots around 3.0 Å resolution. The resolution rings are at 8.8, 4.4, 2.9 and 2.2 Å. (*b*) An image from a crystal of $CKI1_{RD}$ soaked in Paratone-N. The magnified rectangle shows sharp unwidened diffraction spots at a resolution below 2.6 Å. The resolution rings are at 7.9, 3.9, 2.6 and 2.0 Å.

providing us with synchrotron facilities and European Community for support through the Research Infrastructure Action under the FP6 (contract No. RII3/CT/2004/5060008).

References

Bradford, M. M. (1976). *Anal. Biochem.* **72**, 248–254.
Calva, E. & Oropeza, R. (2006). *Microb. Ecol.* **51**, 166–176.
Chang, C. & Stewart, R. C. (1998). *Plant Physiol.* **117**, 723–731.
Cohen, S. X., Ben Jelloul, M., Long, F., Vagin, A., Knipscheer, P., Lebbink, J., Sixma, T. K., Lamzin, V. S., Murshudov, G. N. & Perrakis, A. (2008). *Acta Cryst.* D**64**, 49–60.
Hwang, I. & Sheen, J. (2001). *Nature (London)*, **413**, 383–389.
Hoch, J. A. (2000). *Curr. Opin. Microbiol.* **3**, 165–170.
Kabsch, W. (1993). *J. Appl. Cryst.* **26**, 795–800.
Kakimoto, T. (1996). *Science*, **274**, 982–985.
Keegan, R. M. & Winn, M. D. (2007). *Acta Cryst.* D**63**, 447–457.
Laemmli, U. K. (1970). *Nature (London)*, **227**, 680–685.
Matthews, B. W. (1968). *J. Mol. Biol.* **33**, 491–497.
McCoy, A. J., Grosse-Kunstleve, R. W., Adams, P. D., Winn, M. D., Storoni, L. C. & Read, R. J. (2007). *J. Appl. Cryst.* **40**, 658–674.
Mizuno, T. (2005). *Biosci. Biotechnol. Biochem.* **69**, 2263–2276.
Muller-Dieckmann, H. J., Grantz, A. A. & Kim, S.-H. (1999). *Structure*, **7**, 1547–1556.
Murshudov, G. N., Vagin, A. A. & Dodson, E. J. (1997). *Acta Cryst.* D**53**, 240–255.
Notredame, C., Higgins, D. & Heringa, J. (2000). *J. Mol. Biol.* **302**, 205–217.
Skerker, J. M., Perchuk, B. S., Siryaporn, A., Lubin, E. A., Ashenberg, O., Goulian, M. & Laub, M. T. (2008). *Cell*, **133**, 1043–1054.
Sola, M., Gomis-Ruth, F. X., Serrano, L., Gonzalez, A. & Coll, M. (1999). *J. Mol. Biol.* **285**, 675–687.
Stock, A. M., Mottonen, J. M., Stock, J. B. & Schutt, C. E. (1989). *Nature (London)*, **337**, 745–749.
To, J. P. & Kieber, J. J. (2008). *Trends Plant Sci.* **13**, 85–92.
Tran, L. S., Urao, T., Qin, F., Maruyama, K., Kakimoto, T., Shinozaki, K. & Yamaguchi-Shinozaki, K. (2007). *Proc. Natl Acad. Sci. USA*, **104**, 20623–20628.
Wilcock, D., Pisabarro, M. T., López-Hernandez, E., Serrano, L. & Coll, M. (1998). *Acta Cryst.* D**54**, 378–385.
Yamada, H., Suzuki, T., Terada, K., Takei, K., Ishikawa, K., Miwa, K., Yamashino, T. & Mizuno, T. (2001). *Plant Cell Physiol.* **42**, 1017–1023.